How Does the Electronegativity of the Substituent Dictate the Strength of the Gauche Effect?

C. Thibaudeau, J. Plavec, N. Garg, A. Papchikhin, and J. Chattopadhyaya*

Contribution from the Department of Bioorganic Chemistry, Box 581, Biomedical Centre, University of Uppsala, S-751 23 Uppsala, Sweden

Received November 4, 1993®

Abstract: The distinct conformational preferences observed for the pentofuranosyl moieties in various 3′-substituted 2′,3′-dideoxythymidine derivatives are closely related to the strength of the 3′-gauche effect, which is directly dictated by the electronegativity of the 3′-substituent. The efficiency of the 3′-gauche effect can now be quantitatively calculated with the help of simple linear calibration curves that correlate the gauche effect enthalpy ($\Delta H_{GE}°$) and the group electronegativity (χ) of the 3′-substituent.

Introduction

The pseudorotation concept[1] has been introduced to interpret the spontaneous transitions between indefinite nonplanar geometries of the cyclopentane ring. The Altona–Sundaralingam parameters based on the endocyclic torsion angles are the phase angle of pseudorotation (P), which provides information about the most puckered region of the pentofuranosyl moiety, and the puckering amplitude (ψ_m), which indicates the degree of puckering.[2,3] The survey of 178 X-ray crystal structures of nucleosides and nucleotides[4] has revealed that ribo- and deoxyribofuranosyl moieties occur preferentially within two distinct major conformational regions, referred to as north (N, $0° < P_N < 36°$) and south (S, $144° < P_S < 190°$). In solution, the N and S conformers are involved in a dynamic two-state equilibrium.[3] Earlier, we showed that various steric and stereoelectronic effects of the sugar skeleton (gauche effect) and the nucleobase (anomeric effect) energetically dictate the pseudorotational equilibrium between the two preferred conformational states of the pentofuranosyl moiety in 2′,3′-dideoxynucleosides, 2′-deoxy- and 3′-deoxynucleosides, and ribonucleosides.[5–9] In all 3′-deoxynucleosides, the anomeric and gauche effects are cooperative[8] and maximally achieved in the N sugar conformers, which are therefore strongly preferred owing to favorable pseudoaxial orientations of both the nucleobase and the 2′-OH. However, we have experimentally demonstrated that the presence of a 3′β-Me group on the sugar moiety results in the predominance of the stereoelectronically unfavorable S conformer via intramolecular hydrogen bonding in 3′-deoxy-3′β-methyladenosine.[9] Similarly, we have also shown that the 3′-CH_2OH group on the β-face in 2′,3′-dideoxy-3′-(hydroxymethyl)cytidine preferentially drives the sugar conformation to the S by a sheer steric effect.[6] In 2′-deoxynucleosides, the anomeric and gauche effects are counteractive:[5,8] in N conformers, the nucleobase adopts a pseudoaxial orientation which results in a maximal anomeric effect while the resultant pseudoequatorial location of the 3′-OH group is unfavorable because of the absence of stabilization due to the gauche effect. The situation is however reversed in S pseudorotamers. Nevertheless, the strength of the 3′-gauche effect is stronger than that of the anomeric effect. Therefore, the value of the conformational enthalpy of 2′-deoxynucleosides is negative, which means that the drive of the two state N ⇄ S equilibrium of their sugar moieties is biased toward S pseudorotamers.[5]

The anomeric effect of the nucleobase is thought to originate from the tendency of one of the lone pairs on the endocyclic furanose oxygen to adopt an antiperiplanar orientation relative to the glycosidic bond, whereas the gauche effect is the stabilization of the gauche versus trans orientation in X–C–C–Y fragments upon substitution of X and Y by electronegative groups.[10–12] Hitherto, neither any universal interpretation of the origin of the gauche effect has been formulated nor has any experimental evidence supporting the energetic consequences of the gauche effect been put forward. However, the major influence of the gauche effect has been suggested as due to the stabilization of the bonding–antibonding orbital interactions between vicinal polar bonds.[13] Some authors have also underlined the preponderant role of hydrogen bonding in the preferred gauche orientation of particular O–C–C–O fragments especially in the case of ethylene glycol through *ab initio* molecular orbital calculations (6-311G^{++}G**).[14] Others have shown that the stereoelectronic gauche effect is due to the relative destabilization of the trans conformer, which produces more severely bent bonds and limited bond overlap.[15] In ribonucleosides, there are several types of gauche effects [(O4′–C4′–C3′–O3′), (O3′–C3′–C2′–O2′), (O4′–C1′–C2′–O2′), and (O2′–C2′–C1′–N)] which are involved in the drive of the pseudorotational equilibrium,[5] and therefore it is quite complex to dissect the energetic contribution of any individual gauche effect. This situation is considerably simplified in 2′-deoxynucleosides where a unique gauche effect[16] is operational in the [O4′–C4′–C3′–O3′] fragment, which drives the

* Abstract published in *Advance ACS Abstracts*, March 15, 1994.

(1) Kilpatrick, J. E.; Pitzer, K. S.; Spitzer, R. *J. Am. Chem. Soc.* **1947**, *69*, 2483.
(2) Altona, C.; Sundaralingam, M. *J. Am. Chem. Soc.* **1972**, *94*, 8205.
(3) Altona, C.; Sundaralingam, M. *J. Am. Chem. Soc.* **1973**, *95*, 2333.
(4) de Leeuw, H. P. M.; Haasnoot, C. A. G.; Altona, C. *Isr. J. Chem.* **1980**, *20*, 108.
(5) Plavec, J.; Tong, W.; Chattopadhyaya, J. *J. Am. Chem. Soc.* **1993**, *115*, 9734.
(6) Plavec, J.; Garg, N.; Chattopadhyaya, J. *J. Chem. Soc., Chem. Commun.* **1993**, *12*, 1011.
(7) Plavec, J.; Koole, L. H.; Chattopadhyaya, J. *J. Biochem. Biophys. Methods* **1992**, *25*, 253.
(8) Koole, L. H.; Buck, H. M.; Nyilas, A.; Chattopadhyaya, J. *Can. J. Chem.* **1987**, *65*, 2089.
(9) Koole, L. H.; Buck, H. M.; Bazin, H.; Chattopadhyaya, J. *Tetrahedron* **1987**, *43*, 2289.
(10) Olson, W. K.; Sussman, J. L. *J. Am. Chem. Soc.* **1982**, *104*, 270.
(11) Olson, W. K. *J. Am. Chem. Soc.* **1982**, *104*, 278.
(12) Phillips, L.; Wray, V. *J. Chem. Soc., Chem. Commun.* **1973**, 90.
(13) Brunck, T. K.; Weinhold, F. *J. Am. Chem. Soc.* **1979**, *101*, 1700.
(14) Murcko, M. A.; DiPaola, R. A. *J. Am. Chem. Soc.* **1992**, *114*, 10010.
(15) Wiberg, K. B.; Murcko, M. A.; Laidig, K. E.; MacDougall, P. J. *J. Phys. Chem.* **1990**, *94*, 6956.
(16) The present study cannot however rule out the relative contribution of the steric effect by the 3′-substituent to the drive of pseudorotational equilibrium toward S. Even in acyclic compounds pure 1,4-stereoelectronic interactions based exclusively on the preferred orientation of the lone pairs of 1,4-electronegative substituents can only partly exist. In cyclic compounds, the evaluation of the gauche effect is much more complex because of the following experimentally intractable contributions: (i) steric effect induced by the substituents, (ii) the variable degree of hydration, (iii) the change of hybridization state of the α-carbon.

0002-7863/94/1516-4038$04.50/0

population of the equilibrium between two N and S conformational states of the pentofuranosyl moiety. In both ribo- and 2′-deoxyribonucleosides, the effect of [O5′–C5′–C4′–O4′] is a constant factor in our analysis protocol [5–17,17] (*vide infra*) and therefore it is mutually canceled. It has been experimentally (NMR) demonstrated by us[5–7] that the strengths of the anomeric effect and the gauche effect operating in the [O4′–C4′–C3′–O3′] fragment in 2′-deoxyribonucleosides are dictated by the nature of the heterocyclic base attached to C1′: the anomeric effect decreases from cytosine ≈ uracil ≈ thymine > guanine > adenine, whereas the 3′-gauche effect increases from adenine ≈ cytosine < guanine ≈ thymine.

Some examples are known[8,9,18,19a,20–24] on the qualitative influence of the chemical nature of a 2′- or 3′-substituent on the sugar conformation in nucleosides, but no systematic study has been performed that correlates the electronegativity of various substituents with the position of the pseudorotational equilibrium of 3′-substituted 2′,3′-dideoxynucleosides in thermodynamic terms. We herein report for the first time how the energetics involved in the drive of the N ⇄ S equilibrium are closely connected to the electronic nature of the 3′-substituent.

Results and Discussion

We have examined the $^3J_{HH}$ vicinal coupling constants of a series of potential anti-HIV 2′,3′-dideoxy 3′-substituted thymidine derivatives in which the 3′-substituent has been systematically varied[25] [for **1**, X = H;[26] for **2**, X = NH_2;[27] for **3**, X = OH; for **4**, X = OCH_3;[27] for **5**, X = NO_2;[26] for **6**, X = OPO_3H^-;[27] for **7**, X = F] in order to explore how the polar nature of the 3′-substituent actually influences the drive of the N ⇄ S equilibrium. The question then becomes how can we correlate the electronegativities of various substituents with the thermodynamic properties that drive the pseudorotational equilibrium of the sugar moiety?

Scheme 1. Two-state (north ⇄ south) Pseudorotational Equilibrium in **1–7** [with X = H (**1**), NH_2 (**2**), OH (**3**), OMe (**4**), NO_2 (**5**), OPO_3H^- (**6**), and F (**7**)]

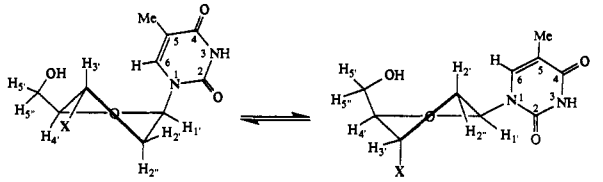

At this stage, it may also be noted that, in each of the 3′-substituted thymidines (Scheme 1), X represents electron-withdrawing groups of varied strengths,[28a–j] while the strengths of the anomeric effect induced by the presence of the thymine base at C1′ and the gauche effect of [O5′–C5′–C4′–O4′] are constant. The strategy of the work is based on a simple rationale that if one detects any difference in the drive of the N ⇄ S conformational equilibrium in the series of compounds **2–7**, relative to 2′,3′-dideoxythymidine (**1**), it can be directly attributed to an alteration of the efficiency of the gauche effect[16] in the [O4′–C4′–C3′–X3′] fragment. Considering 2′,3′-dideoxythymidine **1** as a reference, it is then possible to quantify the gauche effect of each of the above substituents by a simple subtraction procedure, which then quantitatively describes how the gauche effect is influenced by the electronic nature of the 3′-substituent in **2–7**.

Our conformational study of **1–7** is based on the analysis of $^3J_{HH}$ vicinal coupling constants extracted from their ^{1}H-NMR spectra recorded at 500 MHz in D_2O solution between 278 and 358 K in 5 K steps (Table 1 presents the extracted $^3J_{HH}$ in **1–7** at two extreme temperatures) with the assumption of the experimentally observed two-state N ⇄ S equilibrium of the sugar moieties.[17] Subsequently, these experimental couplings have been used as input in the PSEUROT[31] program (version 5.4 based on the λ electronegativity concept[32,33,37]) to calculate their best fit[34] with the conformational parameters (*i.e.* P and ψ_m) and relative populations of the N and S conformers involved in the two-state equilibria of **1–7**, on the basis of the generalized Karplus equation.[32,33,35] The molar fractions of the N (X_N) and S (X_S) conformers obtained from the PSEUROT calculations have been used to make van't Hoff plots of $\ln(X_S/X_N)$ versus $1000/T$ (see Figure 1a for **1–4** and Figure 1b for **5–7**). The average values of $\Delta H°$ and $\Delta S°$ calculated from the slopes and intercepts of individual van't Hoff plots, respectively, and their standard deviations are documented in Table 2.

(17) (a) Previous NMR studies have clearly shown the presence of two distinctly identifiable dynamically interconverting N and S conformations of some sugar moieties in B ⇄ Z DNA[17b,c] or A ⇄ Z RNA[17d,e] or A-form ⇄ B-form lariat RNA[17f,g] transformations as a result of change of the salt or alcohol concentration in the buffer or as a result of change of NMR measurement temperature. These dynamically interconverting N and S sugar pseudorotamers are characterized by only two distinct sets of resonances owing to their different stereochemical environments, and these resonances are also characterized by the typical $^3J_{1'2'}$ coupling constants which are ~0.5 Hz for the N conformer and ~8 Hz for the S conformers. Therefore we have considered only a dynamic two-state N ⇄ S equilibrium because no experimental evidence has ever been reported supporting the existence of a third pseudorotamer in pentose sugar moieties in nucleosides and nucleotides. (b) Feigon, J.; Wang, A. H.-J.; van der Marel, G. A.; van Boom, J. H.; Rich, A. *Nucleic Acids Res.* **1984**, *12*, 1243. (c) Tran-Dinh, S.; Taboury, J.; Neumann, J.-M.; Huynh-Dinh, T.; Genissel, B.; Laglois d'Estaintot, B.; Igolen, J. *Biochemistry* **1984**, *23*, 1362. (d) Davis, P. W.; Hall, K.; Cruz, P.; Tinoco, I.; Neilson, T. *Nucleic Acids Res.* **1986**, *14*, 1279. (e) Davis, P. W.; Adamiak, R. W.; Tinoco, I. *Biopolymers* **1990**, *29*, 109. (f) Agback, P.; Sandstrom, A.; Yamakage, S.-I.; Sund, C.; Glemarec, C.; Chattopadhyaya, J. *J. Biochem. Biophys. Methods* **1993**, *27*, 229. (g) Agback, P.; Glemarec, C.; Yin, L.; Sandstrom, A.; Plavec, J.; Sund, C.; Yamakage, S.-I.; Viswanadham, G.; Rousse, B.; Puri, N.; Chattopadhyaya, J. *Tetrahedron Lett.* **1993**, *34*, 3929.

(18) Rinkel, L. J.; Altona, C. *J. Biomol. Struct. Dyn.* **1987**, *4*, 621.

(19) (a) Plavec, J.; Koole, L. H.; Sandström, A.; Chattopadhyaya, J. *Tetrahedron* **1991**, *47*, 7363. (b) Gurjar, M. K.; Kunwar, A. C.; Reddy, D. V.; Islam, A.; Lalitha, S. V. S.; Jagannadh, B.; Rama Rao, A. V. *Tetrahedron* **1993**, *49*, 4373.

(20) Hossain, N.; Papchikhin, A.; Garg, N.; Fedorov, I.; Chattopadhyaya, J. *Nucleosides Nucleotides* **1993**, *12*, 499.

(21) Glemarec, C.; Reynolds, R. C.; Crooks, P. A.; Maddry, J. A.; Akhtar, M. S.; Montgomery, J. A.; Secrist, J. A., III; Chattopadhyaya, J. *Tetrahedron* **1993**, *49*, 2287.

(22) Guschlbauer, W.; Jankowski, K. *Nucleic Acids Res.* **1980**, *8*, 1421.

(23) Uesugi, S.; Miki, H.; Ikehara, M.; Iwahashi, H.; Kyogoku, Y. *Tetrahedron Lett.* **1979**, 4073.

(24) Klimke, G.; Cuno, I.; Ludemann, H.-D.; Mengel, R.; Robins, M. J. *Z. Naturforsch.* **1979**, *34C*, 1075.

(25) Our data on 3′-azidothymidine[27] (AZT) have not been included in the dataset because H2′ and H2″ protons of AZT are isochronous.[19] However, we have performed its conformational analysis of the basis of $^3J_{HH}$ vicinal couplings at an unstated temperature for 2′α- and 3′β-monodeuterated analogues[19b] of AZT in order to determine limiting $^3J_{HH}$ values of N and S conformers with the help of PSEUROT version 5.4. Three graphical methods[18] were used to back-calculate the molar fractions of the N (X_N) and S (X_S) pseudorotamers from the sums ($^3J_{1'2'} + {}^3J_{1'2''}$), ($^3J_{2'3'} + {}^3J_{2''3'}$), and ($^3J_{2'3'} + {}^3J_{2''3'} + {}^3J_{3'4'}$). The average enthalpy was calculated from the slopes of individual van't Hoff plots ($\Delta H°$ = 1.0 kJ/mol; σ = 0.4), whereas the entropy value calculated from their intercepts was strongly dependent on the selected graphical method ($\Delta S°$ = 2.1 J/(mol K) with σ = 3.2 J/(mol K)).

(26) Garg, N.; Chattopadhyaya, J. Unpublished result.

(27) Papchikhin, A.; Chattopadhyaya, J. Unpublished result.

(28) (a) Wells, P. R. *Prog. Phys. Org. Chem.* **1968**, *6*, 111. (b) Sanderson, R. T. *Chemical Bonds and Bond Energy*, 2nd ed.; Academic Press: New York, 1976; p 41. (c) Huheey, J. E. *J. Phys. Chem.* **1965**, *69*, 3284; **1966**, *70*, 2286. (d) Bratsch, S. G. *J. Chem. Educ.* **1985**, *62*, 101. (e) Inamoto's scale has a strong experimental base: it is closely related to NMR data and claims to describe substituent group effects. The two other scales have been established through theoretical calculations: Marriot's scale is derived from the atomic electron population on the hydrogen atom in H–X compounds, which is estimated by means of a Mulliken population analysis performed on geometries previously optimized by *ab initio* with the 6-31G* basis set. The Mullay's substituent group electronegativities result from orbital electronegativity calculations assuming the principle of partial equalization of the charges along the bonds of the substituent. Note that no group electronegativity for the 3′-OPO_3^- substituent of **6** was available in these three scales. (f) Marriot, S.; Reynolds, W. S.; Taft, R. W.; Thompson, D. *J. Org. Chem.* **1984**, *49*, 959. (g) Mullay, J. *J. Am. Chem. Soc.* **1985**, *107*, 7271. (h) Inamoto, N.; Masuda, S. *Tetrahedron Lett.* **1977**, 3287. (i) Inamoto, N.; Masuda, S.; Tori, K.; Yoshimura, Y. *Tetrahedron Lett.* **1978**, 4547. (j) Inamoto, N.; Masuda, S. *Chem. Lett.* **1982**, *1003*, 1007.

(29) Haasnoot, C. A. G.; de Leeuw, F. A. A. M.; de Leeuw, H. P. M.; Altona, C. *Recl. Trav. Chim. Pays-Bas* **1979**, *98*, 576.

(30) DAISY, Spin Simulation Program, was provided by Bruker.

Table 1. Vicinal Proton–Proton Coupling Constants[a,b] ($^3J_{HH}$) for 1–7 (at Two Extreme Temperatures)

compound	T (K)	$^3J_{1'2'}$	$^3J_{1'2''}$	$^3J_{2'3'}$	$^3J_{2'3''}$	$^3J_{2''3'}$	$^3J_{2''3''}$	$^3J_{3'4'}$	$^3J_{3''4'}$	$^3J_{4'5'}$	$^3J_{4'5''}$
1[c]	278	3.4	7.2	8.4	3.4	10.3	8.4	9.3	6.2	3.0	5.0
	358	4.0	7.2	8.7	4.3	9.3	8.6	8.6	6.5	3.5	5.3
2	278	4.5	7.3	7.9		7.6		6.8		2.8	4.5
	358	4.8	7.3	7.9		7.2		6.5		3.2	4.7
3[c,d]	333	7.0	6.6	6.6		4.2		4.0		3.7	5.1
	358	6.7	6.7	6.9		4.1		4.1		3.8	5.2
4	278	7.9	6.2	6.2		2.8		3.1		3.7	4.7
	358	7.6	6.3	6.3		3.2		3.6		3.9	5.0
5[c,e]	278	7.7	6.4	8.5		3.2		4.1		3.4	4.0
	328	7.5	6.5	8.5		3.4		4.3		3.6	4.3
6[f]	274	7.2	6.5	6.6		3.8		3.7		3.4	4.8
	368	6.7	6.7	7.0		4.4		4.3		3.9	5.1
7	278	9.3	5.6	5.2		1.4		1.3		4.3	4.1
	358	8.8	5.8	5.5		1.7		1.8		g	g

[a] $^3J_{HH}$ values (in Hz, error ±0.1 Hz) have been extracted from one-dimensional ^{1}H-NMR spectra recorded at 500 MHz in D_2O solution between 278 and 358 K in 5 K steps. [b] The populations[29] of the γ^+, γ^-, and γ^t rotamers around the C4′–C5′ bond for 1–7 (at 278 K for 1–5 and 7 and at 274 K for 6) are as follows: for 1, 55%, 6%, and 39%; for 2, 62%, 4%, and 34%; for 3, 48%, 15%, and 37%; for 4, 52%, 15%, and 33%; for 5, 62%, 12%, and 26%; for 6, 54%, 11%, and 35%; and for 7, 53%, 23%, and 24%. [c] The vicinal couplings in 1, 3, and 5 have been obtained through DAISY simulation.[30] [d] The H2′ and H2″ protons in 3 have isochronous chemical shifts below 333 K. Therefore the individual $^3J_{HH}$ could only be extracted through DAISY simulation in the range 333–358 K. [e] 5 was not stable above 328 K. [f] The ^{1}H-NMR spectra of 6 have been recorded between 274 and 368 K at 5 K intervals. [g] Could not be assessed due to identical chemical shifts for H5′ and H5″ in 7 at 358 K.

The absence of any 3′-electron-withdrawing substituent in 2′,3′-dideoxythymidine (1) results in a large positive $\Delta H°$ value (Table 2) which means that the conformational equilibrium is driven to the N conformer. The drive of the pseudorotational equilibrium in 1 originates from the anomeric effect of the thymine base, the substituent effect of the 5′-CH_2OH group, and the steric effect of the nucleobase. The combination of these effects operates maximally when the sugar moiety adopts an N geometry, which is preferred by 84% at 278 K and by 75% at 358 K. The counteracting weaker entropy contribution $-T\Delta S°$ shifts slightly the conformational equilibrium to the S but does not cancel entirely the predominant enthalpy term, so that the free energy remains positive. A parallel can be easily drawn between the conformational behavior of 2′,3′-dideoxythymidine (1) and 2′,3′-dideoxycytidine, 2′,3′-dideoxyadenosine, 2′,3′-dideoxyinosine, and 2′,3′-dideoxyguanosine, which all show[5,7] a preference for the North (≥75% at 278 K) conformer, which is characterized by positive $\Delta H°$ and ΔG^{298}.

The data shown in Table 2 also suggest the influence of the electronic nature of the 3′-substituent effect on the drive of the conformational equilibrium of the pentofuranosyl moiety in 2–7 with respect to 1. Whereas the strong preference observed for N-type sugar conformations in 1 (84% N at 278 K) results essentially from the anomeric effect, the enthalpy driven stabilization of S furanose pseudorotamers in 2–7 [20% S in 2; 64% S in 3 and 6; 74% S in 4; 81% S in 5; and 91% S in 7 at 278 K] can be attributed unambiguously to an increasing preference for gauche orientation of the [O4′–C4′–C3′–X3′] fragment, which progressively prevails over the anomeric effect (Table 2). The relative strengths of the operating gauche effect[16] are quantitatively manifested in the decreasing $\Delta H°$ value of the N ⇄ S equilibrium upon successive substitution of the H3″ in 1 by the electron-withdrawing groups NH_2 (2) > OH (3) > MeO (4) > NO_2 (5) > OPO_3H^- (6) > F (7) (Scheme 1).

At this stage we have quantified the strength of the [O4′–C4′–C3′–X3′] gauche effect in terms of $\Delta H°$ and $\Delta S°$ and analyzed its dependence upon the electronegativity of the 3′-substituent in 2–7. In order to estimate the net influence of the 3′-gauche effect in 2–7, we have calculated the "gauche effect enthalpy" ($\Delta H_{GE}°$) as well as "the substituent effect" (ΔG_{Sub}^{298}) contribution to the global free energy ($\Delta G°$) of the pseudorotational equilibrium, considering 1 as a reference compound (Table 3). The dependence of $\Delta H_{GE}°$ values on the electronic

(31) De Leeuw, F. A. A. M.; Altona, C. *J. Comput. Chem.* **1983**, *4*, 438. PSEUROT, QCPE program no. 463. The program PSEUROT calculates the best fit of the five pseudorotational parameters defining the two-state equilibrium to the set of experimental coupling constants. The user provides the input, which consists of (1) the experimental $^3J_{HH}$ measured at various temperatures, (2) the substituent electronegativities (λ), and (3) the estimated starting values of P_N, P_S, ψ_m^N, ψ_m^S, and the populations of the South Conformer (X_S) at each of the temperatures at which the experimental $^3J_{HH}$ are given. During the iterative optimization procedure on each set (*i.e.* N and S) of starting conformers within a large group of starting geometries (*i.e.* geometries with a wide range of P_N, ψ_N, P_S, and ψ_S; see for example our set of starting geometries on 1–7 in ref 34), one or more conformational parameters can be constrained to assume a fixed value. The PSEUROT program then back-calculates $^3J_{HH}$ for various sets of virtal conformers generated as a function of P_N, P_S, ψ_m^N, ψ_m^S, and X_S and compares it to the experimental $^3J_{HH}$. The quality of the fit is assessed through the calculation of root mean square (rms) deviation between the experimental and the back-calculated $^3J_{HH}$ coupling constants ($\text{rms} = [1/n\Sigma[J_i^{exp} - J_i^{calc}(P_N,\psi_N,P_S,\psi_S,X_S)]^2]^{1/2}$).

(32) Diez, E.; Fabian, J. S.; Guilleme, J.; Altona, C.; Donders, L. A. *Mol. Phys.* **1989**, *68*, 49.

(33) Donders, L. A.; de Leeuw, F. A. A. M.; Altona, C. *Magn. Reson. Chem.* **1989**, *27*, 556.

(34) For the PSEUROT analyses, we have used the following λ electronegativities:[36,37] λ(C1′) = λ(C3′) = λ(C4′) = 0.62; λ(C2′) = 0.67; λ(C5′) = 0.68; λ(O4′) = 1.27. For the 3′-substituents of 1–7: λ(H) = 0.0 (1); λ(NH_2) = 1.10 (2); λ(OH) = 1.26 (3); λ(OMe) = 1.27 (4); λ(NO_2) = 0.77 (5); λ(OPO_3H^-) = 1.27 (6); λ(F) = 1.37 (7). The pseudorotational equilibria of 1, 2, 5, and 7 are strongly biased either to the N (in the case of 1 and 2) or to the S (for 5 and 7) (Table 2). Therefore, PSEUROT fitting processes performed on these compounds without any constraint did not predict reasonable geometries for their minor conformers. In order to take into account the influence of the ill-defined geometry of these minor forms, we have carried out the following set of analyses: for 1 and 2, P_S has been set successively to 150°, 160°, 170°, and 180° (ψ_m^S was fixed at 30°, 35°, and 40°). For 5 and 7, P_N was constrained to −30°, 0°, and +30° with ψ_m^N fixed to 30°, 35°, and 40°. For 4, we have first performed a PSEUROT analysis without any constraint; then we have fixed the geometry of the N conformer (P_N was constrained to −36°, −18°, 0°, +18°, and +36° with ψ_m^N fixed at 31°, 33°, and 35°); at last, ψ_m^N and ψ_m^S have been assumed to be identical and PSEUROT calculations have been performed in the range $30° < \psi_m < 38°$ in 1° resolution, while P_N and P_S were optimized freely. After the PSEUROT fitting process, the major conformers of 1, 2, 4, 5, and 7 have the following optimized geometries: $19° < P_N < 25°$ with $28° < \psi_m^N < 31°$ (1, rms < 0.7 Hz); $32° < P_N < 40°$ with $30° < \psi_m^N < 35°$ (2, rms < 0.6 Hz); for 4, $135° < P_S < 157°$ with $33° < \psi_m^S < 37°$ (P_N and ψ_m^N constrained) and $P_N = -2.8°$, $\psi_m^N = 47.2°$, $P_S = 146.6°$, $\psi_m^S = 28.6°$, for its free PSEUROT analysis (rms < 0.4 Hz); $128° < P_S < 139°$ with $24° < \psi_m^S < 29°$ (5, rms < 0.4 Hz); $156° < P_S < 164°$ with $33° < \psi_m^S < 36°$ (7, rms < 0.3 Hz). 3 and 6 show only a slight preference for the S form. Therefore, their P_N and P_S values were allowed to adjust freely (whereas ψ_m^N and ψ_m^S were both kept fixed to the same value in the range 29–36° for 3 and 30–36° for 6). The P_N and P_S values of the PSEUROT-optimized geometries are as follows: for 3, $4° < P_N < 28°$ and $139° < P_S < 147°$ (rms < 0.3 Hz); for 6, $-8° < P_N < 34°$ and $133° < P_S < 148°$ (rms < 0.4 Hz).

(35) Haasnoot, C. A. G.; de Leeuw, F. A. A. M.; Altona, C. *Tetrahedron* **1980**, *36*, 2783.

(36) Altona, C.; Ippel, J. H.; Westra Hoekzema, A. J.; Erkelens, C.; Groesbeek, M.; Donders, L. A. *Magn. Reson. Chem.* **1989**, *27*, 564.

(37) The electronegativity (λ) dependence of the torsion-angle-independent term in the Karplus–Altona equation, used in the PSEUROT program, has been parametrized by regression analysis using substituent parameters λ^e values scaled according to Huggins electronegativities: $\lambda_H = 0$, $\lambda_{OR} = 1.4$ (see refs 32, 33, and 36 and also the notes by van Wijk, J., and Altona, C., in PSEUROT, version 5.4, July 1992).

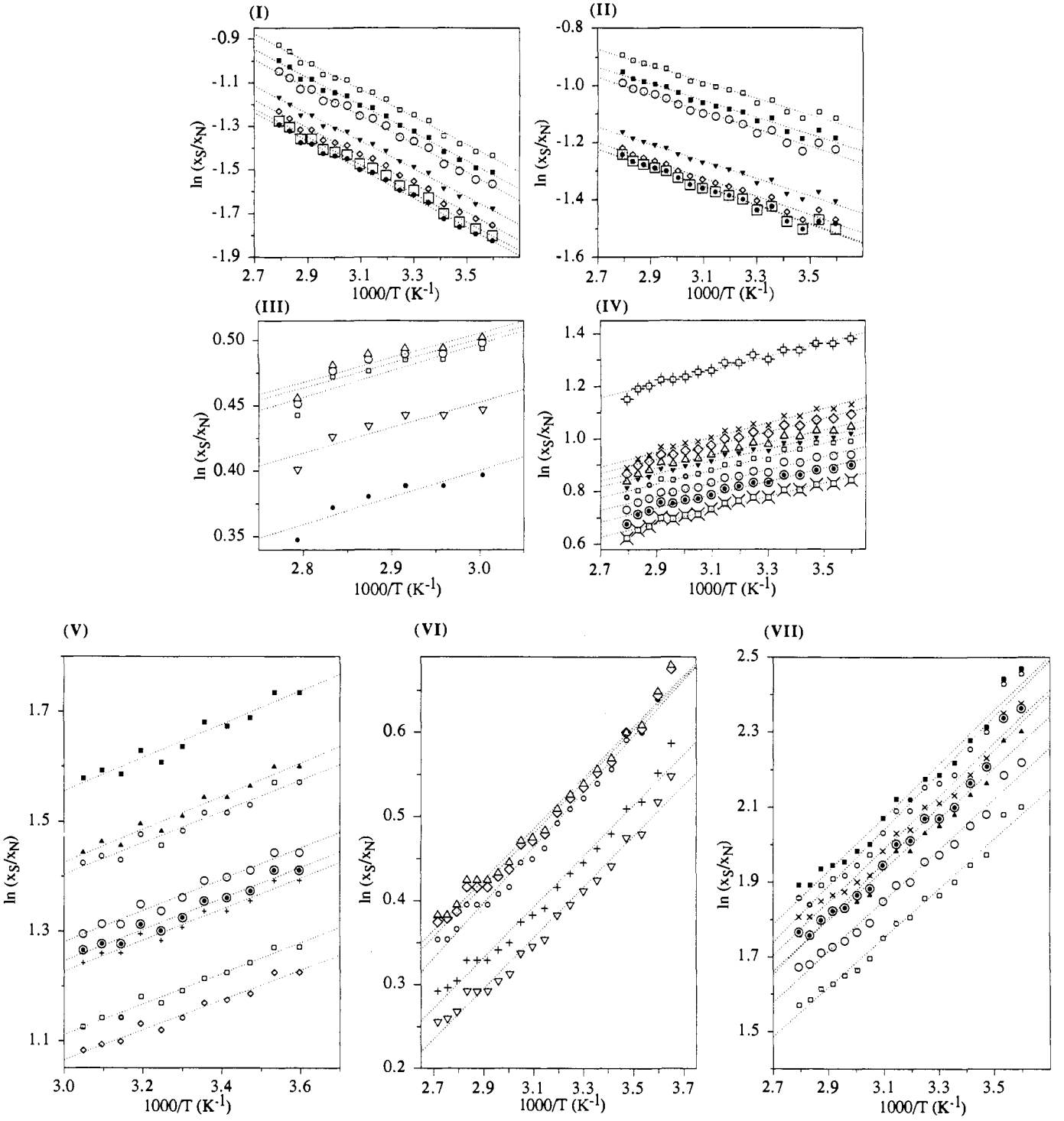

Figure 1. (a, top) van't Hoff plots of $\ln(X_S/X_N)$ versus $1000/T$ for **1** (panel I), **2** (panel II), **3** (panel III), and **4** (panel IV). The straight lines result from least squares fitting processes performed with PROFIT II[38] and are based on the molar fractions of the N (X_N) and S (X_S) conformers from following PSEUROT analyses[34] (for clarity only representative plots are shown): for **1** and **2**, P_S has been constrained to 150° [ψ_m^S = 30° (□), 35° and 40° (▼)], 160° [ψ_m^S = 30° (■), 35° and 40° (◇)], 170° [ψ_m^S = 30° (○), 35° and 40° (□)], and 180° [ψ_m^S = 30°, 35°, and 40° (●)]. For **3**, both ψ_m^N and ψ_m^S were constrained to 29°, 30° (□), 31°, 32°, 33° (○), 34° (△), 35° (▽), and 36° (●) (whereas P_N and P_S were optimized freely). For **4**, we first performed a free PSEUROT analysis (-□-); then further 15 PSEUROT analyses were carried out by constraining P_N to –36° [ψ_m^N = 31°, 33° (○), and 35° (□)], –18° [ψ_m^N = 31°, 33°, and 35°], 0° [ψ_m^N = 31°, 33°, and 35°], 18° [ψ_m^N = 31°, 33°, and 35°], and 36° [ψ_m^N = 31° (⌑),33° (⊙), and 35°]; finally ψ_m^N and ψ_m^S were constrained to identical values in the range 30° < ψ_m < 38° in 1° steps [see the plots of ψ_m^N = 30° (×), 32° (◇), 35° (△), and 36° (▼) in panel IV]. Individual enthalpy ($\Delta H°$) and entropy ($\Delta S°$) values were derived from the slope and intercept, respectively, of each van't Hoff plot, according to the relation $\ln(X_S/X_N) = -(\Delta H°/R)(1000/T) + \Delta S°/R$ and were used to calculate the average $\Delta H°$ and $\Delta S°$ of the N ⇄ S pseudorotational equilibrium in **1**–**4** and their associated standard deviations (σ) (Table 2). (b, bottom) van't Hoff plots of $\ln(X_S/X_N)$ versus $1000/T$ for **5** (panel V), **6** (panel VI), and **7** (panel VII), which gave $\Delta H°$ and $\Delta S°$ of the pseudorotational equilibrium of the sugar moiety in **5**–**7** (see part a and Table 2 for experimental details; for clarity only representative plots are shown). The PSEUROT fitting processes for **5** were performed by constraining P_N to –30° [ψ_m^N = 30° (□), 35° (○), and 40° (▲)], 0° [ψ_m^N = 30° (+), 35° and 40° (■)], and +30° [ψ_m^N = 30° (◇), 35° (⊙), and 40° (○)]. For **6**, we have assumed $\psi_m^N = \psi_m^S$ and constrained them to 30° (○), 31°, 32°, 33° (◇), 34° (△), 35° (+), and 36° (▽) (whereas P_N and P_S were optimized freely). For **7**, P_N has been constrained to –30° [ψ_m^N = 30° (□), 35° (○), and 40° (▲)], 0° [ψ_m^N = 30°, 35° (×), and 40° (■)], and +30° [ψ_m^N = 30°, 35° (⊙), and 40° (○)].

Table 2. Enthalpy and Entropy contributions[a] to the N ⇄ S Pseudorotational Equilibrium of the Pentofuranosyl moiety in **1–7**

compound	ΔH^0 (kJ/mol)	ΔS^0 (J/(mol K))	$-T\Delta S^0$ [b] (kJ/mol)	ΔG^{298} [b] (kJ/mol)	%S[c] (278 K)	%S[c] (358 K)	Δ%S[d] (358–278 K)
1	+5.4 (σ = 0.2)	+6.0 (σ = 0.8)	−1.8	+3.6	16	25	+9
2	+2.6 (σ = 0.1)	−1.9 (σ = 0.7)	+0.6	+3.2	20	25	+5
3	−1.8 (σ = 0.3)	−0.9 (σ = 0.5)	+0.3	−1.5	64	60	−4
4	−2.1 (σ = 0.1)	+1.1 (σ = 0.8)	−0.3	−2.4	74	70	−4
5	−2.4 (σ = 0.1)	+3.7 (σ = 1.1)	−1.1	−3.5	81	78	−3
6	−2.6 (σ = 0.1)	−4.3 (σ = 0.4)	+1.3	−1.3	64	61	−3
7	−5.9 (σ = 0.3)	−2.3 (σ = 0.8)	+0.7	−5.2	91	85	−6

[a] The enthalpy (ΔH^0) and entropy (ΔS^0) contributions to the conformational equilibrium of **1–7** have been averaged (and their associated standard deviations (σ)) from the set of slopes and intercepts of the van't Hoff plots generated by the series of PSEUROT analyses (see ref 34, Figure 1a and b). [b] $-T\Delta S^0$ and ΔG^{298} are given at 298 K. ΔG^{298} has been calculated using the relation $\Delta G^{298} = \Delta H^0 - T\Delta S^0$. [c] The South conformer populations at 278 and 358 K have been back-calculated from the corresponding free energy values as follows: $\%S(T) = 100[\exp(-\Delta G^T/RT)]/[\exp(-\Delta G^T/RT) + 1]$. [d] Δ%S(358–278 K) shows the influence of both the gauche effect enthalpy and entropy contributions.

Table 3. Dependence of the 3′-Gauche Effect Enthalpy (ΔH^0_{GE}) and 3′-Substituent Contributions to the Free Energy ($\Delta G_{Sub}{}^{298}$) upon the Group Electronegativity (χ) of the 3′-Substituent in **2–7**

				group electronegativity (χ) of the 3′-substituent according to[b]		
compound	3′-substituent	ΔH^0_{GE} [a]	$\Delta G_{Sub}{}^{298}$ [a]	Marriot	Mullay	Inamoto
2	NH_2	−2.8	−0.4	0.33	3.15	2.47
3	OH	−7.2	−5.1	0.43	3.97	2.79
4	OMe	−7.5	−6.0	0.44	4.03	2.82
5	NO_2	−7.8	−7.1	0.4	4.08	2.75
6	OPO_3H^-	−8.0	−4.9	0.44 ± 0.1[c]	4.12 ± 0.02[c]	2.8 ± 0.2[c]
7	F	−11.3	−8.8	0.52	4.73	3.1

[a] In kJ/mol; ΔH^0_{GE} and $\Delta G_{Sub}{}^{298}$ have been calculated by subtracting ΔH^0 and ΔG^{298} characterizing the N ⇄ S equilibrium of the sugar moiety in **2–7** from those obtained for **1** (see Table 2). However, no direct correlation could be observed between $\Delta G_{Sub}{}^{298}$ and the 3′-substituent electronegativity. [b] The group electronegativities of the 3′-substituents NH_2 (**2**), OH (**3**), MeO (**4**), NO_2 (**5**), and F (**7**) are given according to ref 28. [c] For **6**, the group electronegativities of the OPO_3H^- substituent have been back-calculated from the ΔH^0_{GE} value using the graphs in Figure 2.

nature of the 3′-substituents in **2–5** and **7** has been examined by the use of various group electronegativity scales derived by Wells,[28a] Sanderson,[28b] Huheey,[28c] Bratsch,[28d] Mullay,[28e,g] Marriot,[28e,f] and Inamoto.[28e,h–j] Mullay *et al.*[28e,g] for the first time showed the interdependence of all group electronegativity scales[28] using Wells' experimental group electronegativity scale[28a] as the reference. This study showed[28e,g] that Mullay's, Marriot's, and Inamoto's group electronegativity scales had the highest correlation coefficients. We have plotted the above electronegativity scales[28a–j] of various 3′-substituents as a function of $\Delta H_{GE}°$ which show that *the magnitude of* $\Delta H_{GE}°$ *increases with the increase of the electronegativity of the 3′-substituent*. This means that the sign of the slope of the plot remains unchanged independent of the group electronegativity scale used.[28a–j] We have evaluated the quality of the above plots for each of the electronegativity scales by calculating the correlation coefficients (R) and the 90% confidence limits of the slopes (S_{90}) and intercepts (I_{90}) with the statistical programs PROFIT[38] and SYSTAT:[39] Wells' scale, R = −0.82, slope = −0.07 (S_{90} = 0.04), intercept = 3.1 (I_{90} = 0.3); Sanderson's scale, R = −0.83, slope = −0.1 (S_{90} = 0.1), intercept = 2.2 (I_{90} = 0.7); Huheey's scale, R = −0.55, slope = −0.2 (S_{90} = 0.2), intercept = 2.3 (I_{90} = 1.9); Bratsch's scale, R = −0.81, slope = −0.2 (S_{90} = 0.1), intercept = 1.6 (I_{90} = 0.9); Mullay's scale, R = −1.0, slope = −0.19 (S_{90} < 0.01), intercept = 2.63 (I_{90} < 0.01); Marriot's scale, R = −0.96, slope = −0.02 (S_{90} = 0.01), intercept = 0.26 (I_{90} = 0.05); Inamoto's scale, R = −0.98, slope = −0.08 (S_{90} = 0.01), intercept = 2.25 (I_{90} = 0.1). Comparison of the above data clearly shows that the three plots based on the scales of Marriot,[28e,f] Mullay,[28e,g] and Inamoto[28e,h–j] give a linear relationship with highest correlation coefficient ($R \geq 0.96$), which is only presented in Figure 2. Table 3 also shows the group electronegativities of the 3′-substituents in **2–5** and **7** according to the electronegativity scales of Marriot,[28e,f] Mullay,[28e,g] and Inamoto,[28e,h–j] whereas the electronegativity of the 3′-substituent of **6** has been calculated from the linear relationships found in the present work between

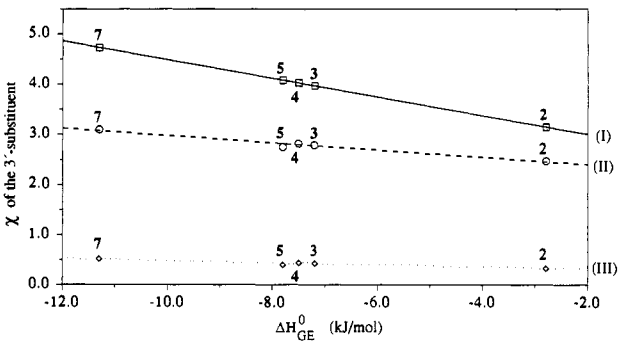

Figure 2. Correlation of the group electronegativity (χ) of the 3′-substituent and the strength of the gauche effect ($\Delta H_{GE}°$) of [O4′–C4′–C3′–X3′] in **2–5** and **7**. Negative $\Delta H_{GE}°$ values denote the drive of the N ⇄ S equilibrium toward S. $\Delta H_{GE}°$ has been calculated by subtraction of the $\Delta H°$ values obtained for **2–5** and **7** from that of **1** (see Tables 2 and 3). The group electronegativities of the 3′-substituents are according to scales derived by Mullay[28g] [solid line I (□)], Marriot[28f] [dashed line II (○)], and Inamoto[28h–j] [dotted line III (◇)]. The equations of the straight lines and the 90% confidence limits of their slopes (S_{90}) and intercepts (I_{90}) have been obtained from least squares fitting procedures performed with the PROFIT program,[38] whereas the Pearson's correlation coefficients (R) have been determined with the SYSTAT program:[39] graph I, Mullay's scale,[28g] $\chi = 2.63 - 0.19\,\Delta H_{GE}°$ (R = −1.0, $S_{90} < 0.01$, $I_{90} < 0.01$); graph II, Marriot's scale,[28f] $\chi = 0.26 - 0.02\Delta H_{GE}°$ (R = −0.96, S_{90} = 0.01, I_{90} = 0.05); graph III, Inamoto's scale,[28h–i] $\chi = 2.25 - 0.08\Delta H_{GE}°$ (R = −0.98, S_{90} = 0.01, I_{90} = 0.1).

electronegativity and $\Delta H_{GE}°$ (*vide infra*). The increase of the electronegativity of the 3′-substituent enhances the strength of the $\Delta H_{GE}°$ driving the N ⇄ S equilibrium toward S. This can be easily rationalized if one considers that the O4′–C4′, C4′–C3′, and C3′–X3′ bonds are more severely bent when the [O4′–C4′–C3′–X3′] fragment is in a trans arrangement; therefore, a gauche orientation is favored as the electronegativity of the substituent (X) increases, which has also been demonstrated by Wiberg *et al.* for 1,2-dihaloethanes.[15] Interestingly, Phillips and Wray had also observed a correlation between the stabilization of the gauche conformer and the sum of Huggins' electronegativities of the halogen atoms[12] on 1,2-dihaloethane in the gas phase. We have

(38) PROFIT II 4.1, Quantum Soft, Postfach 6613, CH-8023 Zürich, Switzerland, 1990.
(39) Wilkinson, L. *SYSTAT*: The System for Statistics; SYSTAT Inc.: Evanston, IL, 1989.

however found no direct correlation between ΔG_{Sub}^{298} and electronegativity (see Table 3), which is most probably due to the fact that the entropy contribution governing the free energy term is dictated by the steric effect of the 3′-substituent.

The result of the straightforward linear relationship between the group electronegativity of the 3′-substituent and its gauche effect ($\Delta H_{GE}°$) on the drive of the pseudorotational equilibrium (Figure 2) is twofold: (1) it is now possible to predict the $\Delta H_{GE}°$ of a 3′-substituent in a nucleoside in aqueous solution if its group electronegativity is known, and conversely, (2) if the $\Delta H_{GE}°$ of the gauche effect driven pseudorotational equilibrium is known, we can easily predict the group electronegativity. Thus, for the first time, it has been found that the group electronegativity of the 3′-phosphomonoester function in the nucleotide **6** is 0.44 in Marriot's scale,[28e,f] 4.12 in Mullay's scale,[28e,g] and 2.8 in Inamoto's scale[28e,h-j] (relative to 3′-OH, 3′-OMe, 3′-F, 3′-NH_2, and 3′-NO_2), which is comparable to the electronegativity of the 3′-NO_2 group (compare their respective $\Delta H_{GE}°$ values in Table 3).

Conclusions

Vicinal proton–proton coupling constants ($^3J_{HH}$) for a series of 3′-substituted 2′,3′-dideoxythymidine derivatives **1–7** were extracted from 500-MHz ^{1}H-NMR spectra recorded between 278 and 358 K in 5 K steps. The temperature-dependent $^3J_{HH}$ were the basis for the conformational analysis of their sugar moieties performed with the PSEUROT[31,34] program. A van't Hoff-type analysis gave $\Delta H°$ and $\Delta S°$ of the two-state pseudorotational N ⇄ S equilibrium in **1–7**. It has been shown that the strong preference for N-type sugar conformations in **1**, resulting essentially from the anomeric effect, is counteracted by the stronger preference of the gauche orientation of the [O4′–C4′–C3′–X3′] fragment. This preference of the gauche effect over the anomeric effect results in the enthalpy driven stabilization of S furanose pseudorotamers in **2–7**. We have furthermore quantitatively estimated the relative strengths of the 3′-gauche effect in **2–7** in terms of enthalpy ($\Delta H_{GE}°$) and found a straightforward linear relationship between the group electronegativity of the 3′-substituents and $\Delta H_{GE}°$. Clearly, the potential application of the above correlation lies in the refinement of the substituent-dependent gauche effect parametrization term in the force field of molecular mechanics and also in the possibility of reparametrization of the electronegativity term in the new generalized Karplus equation. The work in this direction is now in progress in our laboratory.

Experimental Section

^{1}H-NMR Spectroscopy. ^{1}H-NMR spectra were recorded at 500 MHz (Bruker AMX 500) for **1–7** in D_2O (20 mM) between 278 and 358 K at 5 K intervals. All spectra have been recorded using 64K data points and 8 scans. For **3**, however, $^3J_{HH}$ could only be extracted between 333 and 358 K because of isochronicity (see the footnote of Table 1). All assignments have been based on ^{1}H 1D homonuclear decoupling experiments. The non-first-order $^3J_{HH}$ and chemical shifts for **1**, **3**, and **5** were simulated and iterated by the DAISY program package.[30]

Conformational Analyses. The conformational analyses of all nucleosides **1–7** have been performed with the program PSEUROT (version 5.4).[31-33] The λ electronegativities for the substituents in **1–7** are given in ref 34 as well as the results of all PSEUROT analyses.

Acknowledgment. We thank the Swedish Board for Technical Development, Swedish Natural Science Research Council, and Medivir AB, Lunastigen 7, S-141 44 Huddinge, Sweden, for generous financial support. Thanks are due to the Wallenbergstiftelsen, Forskningsrådsnämnden, and University of Uppsala for funds for the purchase of a 500-MHz Bruker AMX NMR spectrometer.